A Novel Method to Synthesize Polystyrene Nanospheres Immobilized with Silver Nanoparticles by Using Compressed CO_2

Jianling Zhang, Zhimin Liu, Buxing Han,* Dongxia Liu, Jing Chen, Jun He, and Tao Jiang[a]

Abstract: In this work, a novel route to synthesize polymer/metal composite nanospheres has been proposed. This method combines the advantages that the polymer chains collapse and entangle in the presence of compressed CO_2, which acts as antisolvent, and the metal nanoparticles and polymers can be precipitated simultaneously from micellar solutions by the easy control of CO_2 pressure. Ag/polystyrene (PS) nanocomposites have been successfully prepared using this method. The transmission electronic micrographs (TEM) of the obtained nanocomposites show that the smaller Ag nanoparticles are immobilized by PS nanospheres of about 50 nm; the phase structure was characterized by X-ray diffraction (XRD). The Ag/PS nanocomposites show absorption properties at a wavelength of $\approx$417 nm. The results of X-ray photoelectron spectra (XPS) and FT-IR spectra indicate that there is no chemical linkage or strong interaction between PS and Ag nanoparticles in the resultant products. This method has many potential advantages for applications and may easily be applied to the preparation of a range of inorganic/polymer composite nanoparticles.

Keywords: carbon dioxide · micelles · nanocomposites · polystyrene · silver

Introduction

In recent years, polymer/inorganic nanocomposites have attracted wide interest in view of their novel properties such as enhanced conductivity,[1] mechanical toughness,[2] and optical[3] and catalytic activity.[4] Different approaches have been used to prepare polymer/metal nanocomposites. The in-situ synthesis of metal nanoparticles in polymer matrices has been widely used.[5] This method is based on the reduction of metal ions that are dispersed in polymer matrices, or the polymerization of the monomer dispersed with the metal nanoparticles. Another route to synthesize the polymer/inorganic nanocomposites is the simultaneous polymerization–reduction approach. The polymerization of the organic monomers was conducted in parallel with the formation of nanocrystalline metal particles by means of γ-irradiation,[6] ultraviolet irradiation,[7] or by radicals directly generated from initiators.[8] Recently, efforts have also been devoted to the synthesis of polymer/inorganic nanocomposites from reverse micelles, during which the polymerizable surfactants were used.[9] Through an in situ polymerization of the surfactants, the inorganic nanoparticles within the micelles could be incorporated into the polymerized matrix.

Currently, there is a great deal of interest on the applications of supercritical (SC) CO_2 in material science.[10] One useful technique is the gas antisolvent process.[11] This technique has been used in different processes, such as extraction and fractionation,[12] recrystallization of chemicals,[13] micronization,[14] and production of polymeric particles.[15] These methods have some potential advantages. For example, it is easy to remove the solvent and antisolvent completely from the products. Moreover, fine particles can be obtained, because high supersaturation can be achieved in the solution, and the morphology of the products can be tuned by the pressure of CO_2.

In previous work, we investigated the thermodynamic nature of polymers in CO_2-expanded solvents.[16] It was revealed that with the addition of CO_2 to solvents, the polymer chains collapse, overlap, and entangle due to prevailing intersegmental attraction in the presence of CO_2. Reverse micelles can be used to synthesize inorganic nanoparticles of different kinds.[17] Recently, we developed a new method to recover the nanoparticles synthesized in reverse micelles by using compressed CO_2 as antisolvent,[18] and ZnS and Ag nanoparticles synthesized in sodium bis(2-ethylhexyl) sulfosuccinate (AOT) reverse micelles were recovered. It was found that, by controlling the pressure of CO_2, the ZnS or Ag nanoparticles synthesized in the reverse micelles could

[a] Dr. J. Zhang, Dr. Z. Liu, Prof. B. Han, Dr. D. Liu, Dr. J. Chen, Dr. J. He, Dr. T. Jiang
Center for Molecular Sciences, Institute of Chemistry
Chinese Academy of Sciences, Beijing 100080 (P.R. China)
Fax: (+86) 10-62559373

 DOI: 10.1002/chem.200305445

be directly precipitated, while the surfactant AOT remains in the solution.

It is interesting and challenging to prepare polymer/metal nanocomposites in which the smaller nanosized metal particles are dispersed in polymer nanospheres, although many approaches have been performed as discussed above. In present work, we have developed a novel route to synthesize polymer/metal nanocomposites, which can be called as reverse-micelle/gas-antisolvent method. The nanospheres of polystyrene (PS) dispersed with the smaller silver nanoparticles have been prepared by using this method. This method combines the four advantages: 1) the size of Ag nanoparticles formed in the AOT/water/cyclohexane reverse micelles is very small;[19] 2) compressed CO_2 can force the Ag nanoparticles to come out of the reverse micelles, while the surfactant AOT remains in the solution;[18] 3) the precipitation of polymers from the solution and the particle morphology and size can be controlled by pressure of CO_2; and 4) the CO_2-expanded solution has low viscosity and high diffusivity, which is favorable for the uniformly dispersion of the silver nanoparticles in the polymer nanospheres. Moreover, the technique is simple, versatile, and timesaving, and the solutions can be recycled. We believe that this method can be used to fabricate a number of nanosized composites consisting of inorganic nanoparticles and polymers with unique advantages.

The principle of this method is shown in Figure 1. The inorganic nanoparticles are first synthesized in the AOT/water/cyclohexane reverse micelles, and the polymer is then

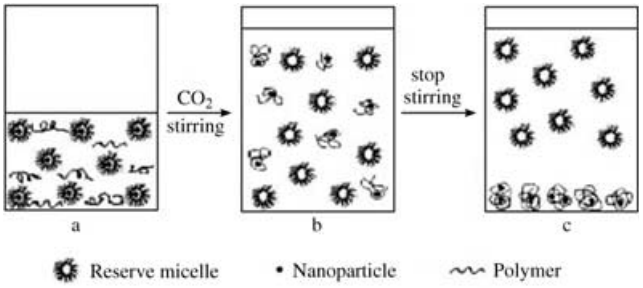

Figure 1. Scheme for the synthesis of silver/polystyrene nanocomposites from the micellar solutions.

dissolved in the solution (Figure 1a). CO_2 is added and the solution is stirred. The metal nanoparticles come out from the reverse micelles at suitable pressure of CO_2.[18] At the same time, CO_2 causes the polymer chains to collapse, overlap, and entangle, because CO_2 acts as an antisolvent.[16] During this process, the inorganic nanoparticles are absorbed, trapped, or wrapped to form the nanocomposite (Figure 1b). Then the stirrer is stopped and the composites precipitate (Figure 1c). After releasing solution, the precipitates are collected.

Experimental Section

Material: CO_2 (>99.995% purity) was provided by Beijing Analysis Instrument Factory. The monodisperse polystyrene was synthesized by Nanjing Chemical Engineering University, of which the molecular weight was $M_w = 22400$ ($M_w/M_n = 1.05$, $D = 1.04\ g\,cm^{-3}$). The surfactant AOT was purchased from Sigma with purity of 99%. The solvent cyclohexane was purchased from Beijing Chemical Factory (>99.5%) and used as received. KBH_4, $AgNO_3$, and ethanol, supplied by Beijing Chemical Plant, were all A.R. grade. Double-distilled water was used.

Volume expansion of CO_2–micellar solution system: The apparatus for determining the expansion curves of the AOT/cyclohexane solution ($[AOT] = 50\ mmol\,L^{-1}$)in CO_2 was the same as that reported previously.[18] In a typical experiment, AOT/cyclohexane solution (10 mL) was charged into the view cell. CO_2 was then charged into the view cell to a suitable pressure after thermal equilibrium had been reached. A magnetic stirrer was used to enhance the mixing of CO_2 and the solution. The volume of the liquid phase did not change with time after equilibrium was reached. The pressure and the volume at equilibrium condition were recorded. More CO_2 was added and the volume of the liquid phase at another pressure was determined. The volume expansion coefficients were calculated on the basis of the liquid volumes before and after dissolution of CO_2. Some surfactant could be precipitated when the pressure of CO_2 was high enough. The pressure at which the surfactant begins to precipitate is called as cloud point pressure. The cloud point pressure of the solution was also determined.

Synthesis of Ag nanoparticles in micellar solutions containing PS: The procedures to synthesize Ag nanoparticles in reverse micelles were similar to that reported by other authors.[20] The solution of AOT in cyclohexane was first prepared ($[AOT] = 50\ mmol\,L^{-1}$). Then reverse micellar solutions containing aqueous solutions of $AgNO_3$ and KBH_4 were prepared by adding corresponding aqueous salt solution ($[AgNO_3] = 2[KBH_4] = 0.4\ mol\,L^{-1}$) to the surfactant solution; the molar ratio of water to AOT (w) was 5. The two micellar solutions containing $AgNO_3$ and KBH_4, respectively, were mixed and silver nanoparticles were formed in the reverse micelles due to the water pools can exchange their contents by a collision process.[21] Then the suitable amount of PS was dissolved in the micellar solution ($[PS]_0 = 1.88\ mg\,mL^{-1}$).

High-pressure UV-visible spectra: The key of this method is to precipitate the Ag particles in the reverse micelles and the PS in the solution simultaneously by the use of compressed CO_2, while the AOT remains in the solution. Therefore, we first tested this by UV-visible spectroscopy. The apparatus and procedures for the UV-visible experiments were similar to those described previously.[18] In a typical experiment, the desired amount of the reverse micellar solutions containing the Ag nanoparticles and PS was added into the temperature-controlled high-pressure UV cell. After the thermal equilibrium had been reached, CO_2 was charged into the cell by high-pressure pump until the cell was full. The UV spectrum of the solution was recorded every 10 minutes until it was unchanged, which was an indication of equilibrium condition.

Synthesis of Ag/PS composite particles: The Ag/PS nanocomposites were synthesized as follows. Reverse micellar solutions (30 mL) containing the Ag nanoparticles and PS synthesized as above was loaded into a cylinder-shaped autoclave of 120 mL. The autoclave was put in a thermostat, and CO_2 was charged by a high-pressure pump until the desired pressure was reached. The solution was stirred (400 r.p.m.) for 1 h, then the stirrer was stopped and the nanocomposites were precipitated. After releasing solution, the precipitates were collected and washed by water and ethanol several times. The products were dried under vacuum at 303.2 K for 4 h.

Characterization: The morphologies of the obtained particles were determined by TEM with a TECNAI 20 PHILIPS electron microscope. Particles were dispersed in ethanol and then directly deposited on the copper grid. X-ray diffraction analysis of the samples was carried out using an X-ray diffractometer (XRD, Model D/MAX2500, Rigaka) with $Cu_{K\alpha}$ radiation. For UV-visible absorption investigation, a certain amount of the obtained Ag/PS powders were dispersed in ethanol and determined by a TU-1201 model spectrophotometer. X-ray photoelectron spectra (XPS) were collected by means of an ESCALab220i-XL spectrometer at a pressure of about 3×10^{-9} mbar with $Al_K\alpha$ as the exciting source ($h\nu = 1486.6$ eV) and operating at 15 kV and 20 mA. The IR spectrum was recorded using an IR spectrometer (TENSOR 27), and each sample was recorded with 32 scans at an effective resolution of $2\ cm^{-1}$.

Results and Discussion

Volume expansion of CO_2–micellar solution system: The micellar solution expands after dissolution of CO_2. The volume expansion coefficient ΔV ($\Delta V = (V - V_0)\,V_0$, in which V and V_0 are the volumes of the CO_2-expanded and CO_2-free solution, respectively) of the solution at different CO_2 pressures is a very important parameter for the UV experiments and the co-precipitation process. We determined the ΔV of the AOT/cyclohexane solution ([AOT] = 50 mmol L^{-1}) in CO_2 at two temperatures, namely 301.2 and 307.2 K (Figure 2). Evi-

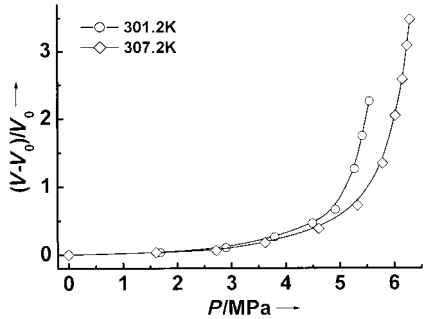

Figure 2. Expansion curves of AOT/cyclohexane solution ([AOT] = 50 mmol L^{-1}) at different temperatures and pressures.

dently, ΔV increases with increasing pressure, and it is more sensitive to pressure in the high-pressure range. The ΔV at the lower temperature is larger provided pressure is the same. The cloud-point pressure of the AOT/cyclohexane solutions ([AOT] = 50 mmol L^{-1}) was calculated as 5.58 and 6.32 MPa at 301.2 and 307.2 K, respectively. All the experiments were conducted at pressures lower than the cloud point pressure for the UV spectrum determination and recovery process, so the precipitation of the surfactant did not occur.

UV studies on the coprecipitation of Ag and PS: Colloidal dispersions of silver exhibit absorption bands in the UV-visible range that are due to the resonant excitation of surface plasmons. Thereby the silver nanoparticles stabilized in the reverse micelles can be analyzed in situ by UV-visible spectra.[22] The characteristic absorption spectrum for silver nanoparticles has a peak at about 400 nm. The Ag nanoparticles solubilized in the reverse micelles and the PS dissolved in the solution do not precipitate in the absence of CO_2. The possibility to precipitate the Ag nanoparticles in the reverse micelles and the polymer in the solutions simultaneously by using CO_2 was investigated by UV-visible spectroscopy. The results show that this can be achieved at suitable conditions. As an example, Figure 3 illustrates the UV spectra of reverse micellar solution containing the Ag nanoparticles and PS at 307.2 K and at some typical pressures. For all the experiments, the concentrations of Ag and PS in the reverse micellar solutions after expansion should be 0.025 and 1.88 mg mL^{-1}, respectively, if they are not precipitated. Evidently, the intensity of the absorption bands for Ag and PS (at about 260 nm) decreases gradually with increasing pres-

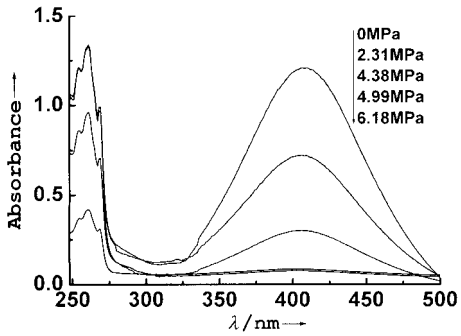

Figure 3. UV spectra of a micellar solution containing Ag and PS at 307.2 K and different CO_2 pressures.

sure, indicating the precipitation of Ag and PS. Our experiments showed that the absorbance of silver and PS is a linear function of Ag and PS concentration as their concentrations are lower than 0.03 mg mL^{-1} and 2.0 mg mL^{-1}, respectively. Thus the precipitation percentage of Ag and PS can be calculated from the absorbance. Figure 4 shows the

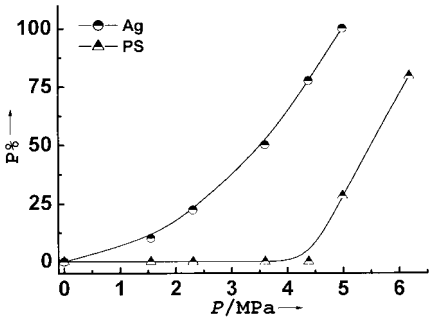

Figure 4. Precipitation percentage of Ag (P_{Ag}%) and PS (P_{PS}%) from micellar solutions at 307.2 K and different pressures.

dependence of precipitation percentage of Ag and PS (the mass of the precipitated Ag or PS divided by the total mass of Ag or PS, respectively) on CO_2 pressure. Ag particles precipitate gradually with increasing pressure, while PS begins to precipitate at about 4.99 MPa. As the pressure reaches 6.18 MPa, which is lower than the pressure (6.32 MPa) at which the surfactant AOT begins to precipitate at this temperature, the precipitation percentage of Ag reaches 100% and that of PS is about 80%. This illustrates that all Ag and most of the PS can be precipitated under these conditions, while the surfactant remains in the solution. In other words, the co-precipitation of Ag and PS from the micellar solutions can be accomplished by controlling the pressure of CO_2, and it is expected that the composition of the obtained Ag/PS nanocomposites can be tuned by controlling pressure. On the basis of the results above, we synthesized the Ag/PS nanocomposites under different conditions.

Morphologies of Ag/PS nanocomposites: The transmission electronic micrographs (TEM) of pure Ag nanoparticles recovered from the reverse micelles, PS obtained from cyclo-

hexane, and the Ag/PS nanocomposites fabricated at different conditions are shown in Figure 5a–e. As we can see, spherical Ag particles of about 3 ± 1 nm in diameter (shown in Figure 5a) and PS nanospheres with diameter of about

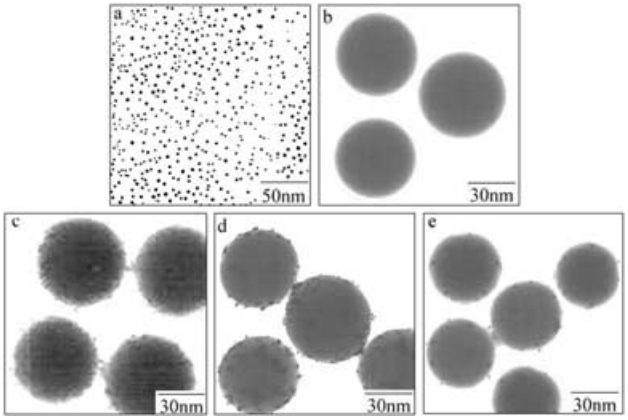

Figure 5. TEM photographs of a) pure silver recovered from the AOT reverse micelles and b) PS recovered from cyclohexane obtained at 5.50 MPa and 307.2 K; c)–e) show the TEM photographs of the Ag/PS nanocomposites obtained at: 5.50 MPa and 301.2 K (c); 5.50 MPa, 307.2 K (d); 6.28 MPa and 307.2 K (e).

50 nm (shown in Figure 5b) are obtained at 5.50 MPa and 307.2 K, respectively. For the Ag/PS nanocomposites shown in Figure 5c–e, it is evident that the Ag nanoparticles are immobilized by the polymer nanospheres. And by increasing the temperature and pressure, the particles size is decreased from about 65 nm (shown in Figure 5c), to 55 nm (shown in Figure 5d) to 40 nm (shown in Figure 5e). The physical coalescence of nanoparticles may be responsible for this phenomenon. As the pressure and temperature is increased, the solution is less viscous and diffusivity is larger; this enhances the degree of molecular mobility and reduces the contact time of the particles as they collide. This may reduce the physical coalescence of nanoparticles. Therefore, smaller particles are obtained at higher pressure and temperature. Moreover, it can be seen from Figure 5 that with the increase of CO_2 pressure, the number of the silver nanoparticles immobilized by per PS sphere is decreased. The content of silver in the composites can be estimated by analyzing the XPS results. For example, the atom ratios of silver to carbon are 0.0078/1 and 0.0059/1 for silver/PS composites prepared at 5.50 and 6.28 MPa (307.2 K), respectively. The reason is that the Ag particles can be precipitated completely at the experimental pressures, while the precipitation percentage of the PS increases with increasing pressure, as discussed above. Thus through the easy control of experimental conditions, the composition and size of the composite nanospheres can be tuned.

We also estimated roughly the atom ratio of Ag on the surface of a PS sphere to C in the sphere from the TEM micrograms; for this we used the diameter of Ag particles on the surface of PS sphere, the diameter of the PS sphere, and the densities of Ag ($10.5\,g\,cm^{-3}$) and PS ($1.04\,g\,cm^{-3}$). The Ag/C ratios estimated from TEM micrographs of the composites prepared at 5.50 MPa and 6.18 MPa at 307.2 K (Figure 5d and e) are 0.0004/1 and 0.0002/1, respectively, which are much smaller than those obtained from XPS measurements, indicating that most Ag particles exist inside PS spheres.

Additional characterization: The phase structure of the obtained product was characterized by X-ray diffraction (XRD). As examples, Figure 6 shows the pattern of the composite prepared at 5.50 MPa and 301.2 K and that of PS.

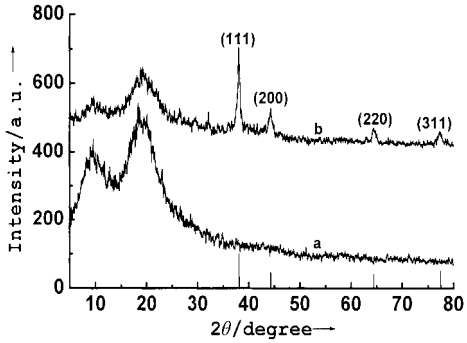

Figure 6. X-ray diffraction patterns of a) pure PS and b) Ag/PS nanocompsites obtained at 5.50 MPa and 301.2 K. The vertical lines at the bottom indicate the standard positions and relative intensities of fcc silver.

Besides the diffraction of PS phase (curve a), the Ag/PS composites exhibit four peaks (curve b) corresponding to the face center cubic (fcc) Ag phase (111, 200, 220, 311) with cell parameter $a=0.4099$ nm, which is close to the reported data (JCPDS File No. 4-0783). The broadening of the peaks suggests the presence of very small Ag particles.

UV-visible spectra were used to characterize the absorption properties for the Ag/PS composites, and the results are shown in Figure 7. Pure PS has no absorption at the wave-

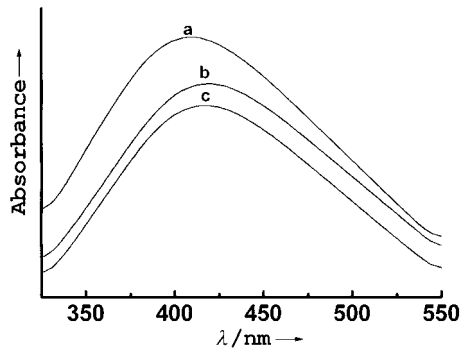

Figure 7. UV-visible spectra of a) pure Ag obtained at 5.50 MPa, 301.2 K, and of Ag/PS composite obtained at b) 5.50 MPa, 301.2 K and c) 6.28 MPa, 307.2 K.

length around 400 nm. As shown in the figure, the Ag/PS nanocomposite in ethanol displays a strong absorption band at about 417 nm, which is attributed to the surface plasmon excitation of the silver particles.[23] In contrast to the absorb-

ance of pure silver ($\lambda_{max} = 409$ nm), the absorption is red-shifted upon incorporation of Ag nanoparticles into PS. This may be due to the agglomeration of the Ag nanoparticles and/or change of the dielectric properties of the surrounding environment.[24]

To obtain the information about the interfacial interaction between Ag nanoparticles and the polymer matrices, X-ray photoelectron spectra (XPS) measurements of the composites were conducted and the results are illustrated in Figure 8. Neat PS shows an intense C 1s peak at 284.6 eV

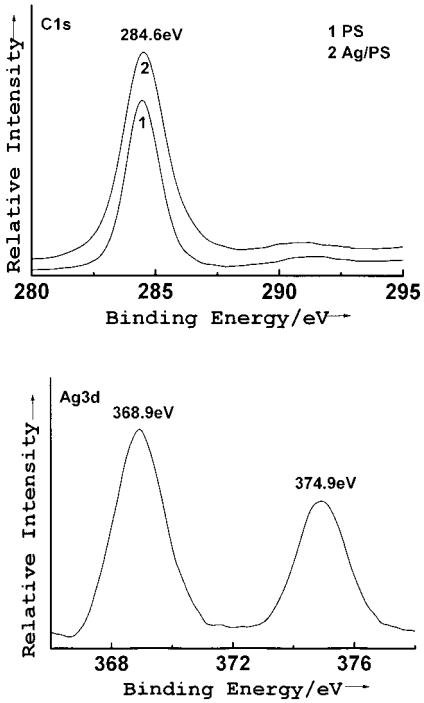

Figure 8. C 1s (top) and Ag 3d (bottom) XPS spectra of PS and Ag/PS nanocomposite obtained at 5.50 MPa and 301.2 K.

and the characteristic π–π* shakeup satellite peak of the phenyl rings is observed between 290 and 292 eV.[25] Figure 8 (top) indicates that the C 1s peak of Ag/PS composites is almost unchanged, which might suggest that there is no strong interaction between Ag and PS matrix. The Ag 3d core level XPS spectrum of Ag/PS is shown at the bottom of Figure 8. The Ag 3d doublet at 368.9 and 374.9 eV is assigned to Ag $3d_{5/2}$ and Ag $3d_{3/2}$, respectively. The binding energy (BE) maximum of Ag $3d_{5/2}$ is 0.6 eV higher than that of Ag in the literature (368.3 eV).[26] However, the intensity ratio of the Ag 3d doublet is near 1.5 and the difference in the BE maximum, that is, spin-orbit splitting, is about 6.0; these values agree well with those in the literature.[26] The shift of Ag $3d_{5/2}$ peak to higher binding energies may be attributed to the oxidation of surface silver atoms.[23d]

FTIR spectra of nanocomposites also give information on the interfacial interaction between silver and the polymer matrices. Figure 9 displays the IR spectrum of pure PS and the Ag-nanoparticle-filled PS dispersed in KBr matrices. As shown in the figure, the vibrational bands typical for PS, such as C–H aromatic and aliphatic stretching at 3100–

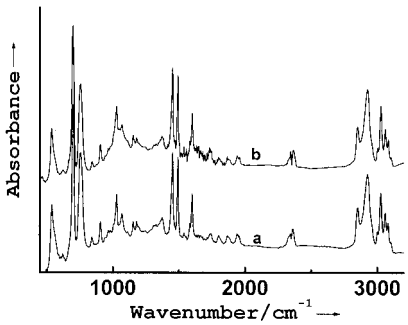

Figure 9. IR spectra of a) pure PS samples and b) Ag/PS nanocomposite obtained at 5.50 MPa and 301.2 K.

2800 cm^{-1} and C=C vibrations at 1492 cm^{-1} and 1452 cm^{-1}, are clearly observed. The two spectra are identical. This implies that there is no chemical linkage or strong interaction between PS and silver nanoparticles in the resultant products; this is consistent with the results of XPS measurements.

Conclusion

In summary, this work describes a route to synthesize the silver/polystyrene nanocomposites by the antisolvent technique combined with the reverse micelle method. The nanospheres of polystyrene dispersed with the smaller silver nanoparticles are obtained. The size and composition of the composite nanospheres can be controlled by the experimental conditions, such as the CO_2 pressure and temperature. Moreover, this method has some potential advantages for applications as it is simple, timesaving, and the solutions can be recycled. This process may easily be applied to a range of inorganic/polymer composite nanoparticles with different size and compositions.

Acknowledgement

The authors are grateful to the National Natural Science Foundation of China (20374057,20133030).

[1] a) E. Coronado, J. R. Galan-Mascaros, C. J. Gomez-Garcia, V. Laukhin, *Nature* **2000**, *408*, 447; b) R. Gangopadhyay, A. De, *Chem. Mater.* **2000**, *12*, 608; c) H. Xia, Q. Wang, *Chem. Mater.* **2002**, *14*, 2158.

[2] a) T. J. Pinnavaia, *Science* **1983**, *220*, 365; b) Y. Li, J. Yu, Z. X. Guo, *J. Appl. Polym. Sci.* **2002**, *84*, 827.

[3] a) Y. Wang, N. Herron, *Science* **1996**, *273*, 632; b) M. R. Bockstaller, E. L. Thomas *J. Phys. Chem. B* **2003**, *107*, 10017; c) H. Du, G. Q. Xu, W. S. Chin, L. Huang, W. Ji, *Chem. Mater.* **2002**, *14*, 4473.

[4] a) S. N. Sidorov, I. V. Volkov, V. A. Davankov, M. P. Tsyurupa, P. M. Valetsky, L. M. Bronstein, R. Karlinsey, J. W. Zwanziger, V. G. Matveeva, E. M. Sulman, N. V. Lakina, E. A. Wilder, R. J. Spontak, *J. Am. Chem. Soc.* **2001**, *123*, 10502; b) I. Hussain, M. Brust, A. J. Papworth, A. I. Cooper, *Langmuir* **2003**, *19*, 4831; c) A. N. Shipway, I. Willner, *Chem. Commun.* **2001**, 2035.

[5] a) D. W. Hatchett, M. Josowicz, J. Janata, D. R. Baeer, *Chem. Mater.* **1999**, *11*, 2989; b) A. B. R. Mayer, W. Grebner, R. Wannemacher, *J. Phys. Chem. B* **2000**, *104*, 7278.

[6] Y. Zhu, Y. Qian, X. Li, M. Zhang, *Chem. Commun.* **1997**, 1081.

[7] Z. P. Zhang, L. D. Zhang, S. X. Wang, W. Chen, Y. Lei, *Polymer* **2001**, *42*, 8315.
[8] C.-W. Chen, M.-Q. Chen, T. Serizawa, M. Akashi, *Adv. Mater.* **1998**, *10*, 1122.
[9] a) M. Summers, J. Eastoe, *Adv. Colloid Interface Sci.* **2003**, *100*, 137; b) T. Hirai, T. Watanabe, I. Komasawa, *J. Phys. Chem. B* **2000**, *104*, 8962; c) R. A. Mackay, F. M. Pavel, *Langmuir* **2000**, *16*, 8568.
[10] a) J. M. DeSimone, *Science* **2002**, *297*, 799; b) A. I. Cooper, *Adv.Mater.* **2001**, *13*, 1111.
[11] E. Reveerchon, *J. Supercrit. Fluids* **1999**, *15*,1.
[12] a) M. A. Winters, D. Z. Frankel, P. G. Debenedetti, J. Carey, M. Devaney, T. M. Przybycien, *Biotechnol. Bioeng.* **1999**, *62*, 247; b) F. Favari, A. Bertucco, N. Elvassore, M. Fermeglia, *Chem. Eng. Sci.* **2000**, *55*, 2379.
[13] M. Muller, U. Meier, A. Kessler, M. Mazzotti, *Ind. Eng. Chem. Res.* **2000**, *39*, 2260.
[14] M. Sarkari, I. Darrat, B. L. Knutson, *AIChE J.* **2000**, *46*, 1850.
[15] a) D. J. Dixon, G. Lunabarcenas, K. P. Johnston, *Polymer* **1994**, *35*, 3998; b) D. Li, Z. M. Liu, G. Y. Yang, B. X. Han, H. K. Yan, *Polymer* **2000**, *41*, 5707.
[16] a) D. Li, .B. X. Han, Z. M. Liu, J. Liu, X. G. Zhang, S. G. Wang, X. F. Zhang, J. Wang, B. Z. Dong, *Macromolecules* **2001**, *34*, 2195; b) D. Li, B. X. Han, Q. Huo, J. Wang, B. Z. Dong, *Macromolecules*, **2001**, *34*, 6721.
[17] a) D. B. Zhang, H. M. Cheng, J. M. Ma, Y. P. Wang, X. Z. Gai, *J. Mater. Sci. Lett.* **2001**, *20*, 439; b) F. T. Quinlin, J. Kuther, W. Tremel, W. Knoll, S. Risbud, P. Stroeve, *Langmuir* **2000**, *16*, 4049; c) F. Agnoli, W. L. Zhou, C. J. O'Connor, *Adv. Mater.* **2001**, *13*, 1697; d) R. Bsndyopadhyaya, R. Kumar, K. S. Gandhi, *Langmuir* **2000**, *16*, 7139; e) C. Petit, A. Taleb, M. P. Pileni, *Adv. Mater.* **1998**, *10*, 259; f) E. Stathatos, P. Lianos, F. D. Monte, D. Levy, D. Tsiourvas, *Langmuir* **1997**, *13*, 4295.
[18] a) J. L. Zhang, B. Han, J. C. Liu, X. G. Zhang, J. He, Z. M. Liu, *Chem.Commun.* **2001**, 2724; b) J. L. Zhang, B. Han, J. C. Liu, X. G. Zhang, J. He, Z. M. Liu, T. Jiang, G. Y. Yang, *Chem. Eur. J.* **2002**, *8*, 3879.
[19] M. P. Pileni, T. Zemb, C. Petit, *Chem. Phys. Lett.* **1985**, *118*, 414.
[20] P. Barnickel, A. Wokaun, W. Sager, H. F. Eicke, *J. Colloid Interface Sci.* **1992**, *148*, 80.
[21] P. D. I. Fletcher, A. M. Howe, B. H. Robinson, *J. Chem. Soc. Faraday Trans. 1* **1987**, *83*, 985.
[22] a) J. P. Cason, K. Khambaswadkar, C. B. Roberts, *Ind. Eng. Chem. Res.* **2000**, *39*, 4749; b) M. Ji, X. Chen, C. M. Wai, J. L. Fulton, *J. Am. Chem. Soc.* **1999**, *121*, 2631; c) C. Petit, P. Lixon, M. P. Pileni, *J. Phys. Chem.* **1993**, *97*, 12974; d) J. A. Greighton, D. G. Eaton, *J. Chem. Soc. Faraday Trans.* **1991**, *87*, 3881.
[23] a) S. M. Marinakos, M. F. Anderson, J. A. Ryan, L. D. Martin, D. L. Feldheim, *J. Phys. Chem. B* **2001**, *105*, 8872; b) T. Ung, M. Giersig, D. Dunstan, P. Mulvaney, C.-W. Chen, T. Serizawa, M. Akashi, *Langmuir* **1997**, *13*, 1773; c) F. Mafune, J.-y. Kohno, Y. Takeda, T. Kondow, H. Sawabe, *J. Phys. Chem. B.* **2000**, *104*, 8333; d) C.-W. Chen, T. Serizawa, M. Akashi, *Langmuir* **1999**, *15*, 7998.
[24] Z. H. Mbhele, M. G. Salemane, C. G. C. E. van Sittert, J. M. Nedeljković, V. Djoković, A. S. Luyt, *Chem. Mater.* **2003**, *15*, 5019.
[25] a) G. Beamson, D. Briggs, High-Resolution XPS of Organic Polymers, The Scienta ESCA300 Database; b) R. M. France, R. D. Short, *Langmuir* **1998**, *14*, 4827; c) S. B. Idage, S. Badrinarayan, *Langmuir* **1998**, *14*, 2780; d) H. Sertchook, D. Avnir, *Chem. Mater.* **2003**, *15*, 1690.
[26] J. F. Moulder, W. F. Stickle, P. E. Sobol, K. D. Bomben, in *Handbook of X-ray Photoelectron Spectroscopy* (Ed.: J. Chastain), Perkin–Elmer Corporation, Eden Prairie, MN, **1992**, p. 120.

Received: August 13, 2003
Revised: January 13, 2004
Published online: May 25, 2004

